Introduction

Tunnelling all over the world often utilizes tunnel boring machines (TBMs). This way of tunnel excavation limits disturbances to the surrounding host rock, which is especially important in urban areas. Also, it increases the overall tunnel construction performance and reduces the cost of lining the tunnel by providing a smooth tunnel wall. TBMs are capable of drilling through almost all kind of rocks, and the geological situation along the tunnel profile is usually well known (Lüth et al., 2006). However, geological mapping based on surface measurements and geophysical data lack resolution with increasing depth. Hence, there can be uncertainties regarding the location or even the existence of geological structures ahead of the tunnel construction. Look-ahead prediction methods can help to decrease these uncertainties by correlating assumed geological features with their actual spatial location. Thereby, expensive TBM downtimes and safety risks can be minimized, too.

We recently introduced a seismic tunnel look-ahead prediction method using tunnel surface-waves (Bohlen et al., 2007, Jetschny et al., 2009). Without interference in the tunnel construction, tunnel surface-waves (TS-waves) are excited behind the TBM and travel along the tunnel wall in drilling direction (see Figure 1). At the tunnel face, these TS-waves are mainly converted into body S-waves which can be reflected at geological heterogeneities ahead of the tunnel. After re-conversion at the tunnel face as TS-waves, these seismic signals can be recorded by receivers placed behind the TBM, and provide information on the distance and the spatial location of the reflector. According to its wave path, as both a direct TS-wave, converted S-wave, reflected S-wave and back-converted TS-wave, we call these signals TSST-waves, even though TS-S-S-TS-wave would be the more precise term. At different tunnel construction sites the look-ahead prediction using TSST-waves has proven its capability of imaging fault zones, lithological interfaces and other geological structures (Bohlen et al., 2007, Lüth et al., 2006).

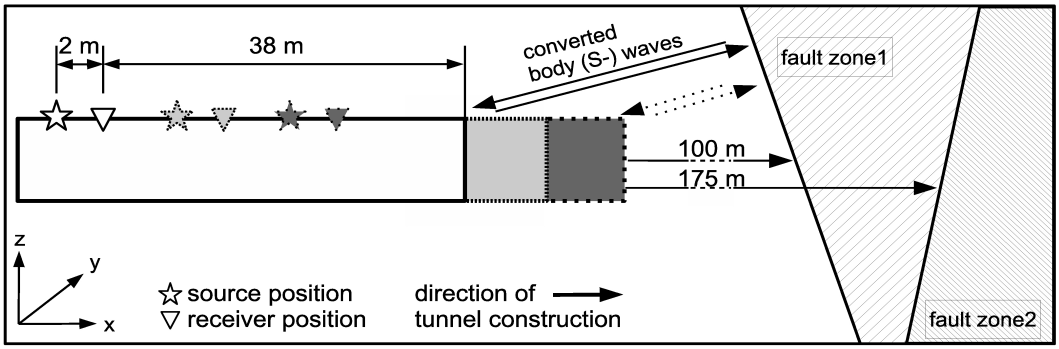

Figure 1: *Schematic measurement geometry for a tunnel look-ahead prediction survey. Sources and receivers are marked by stars and a triangles, respectively. While the tunnel construction is approaching the fault zone, the measurement geometry is moving, too.*

Imaging processing scheme

Regardless of the method, current interpretation of tunnel seismic data requires in most cases either an experienced geophysicist present on the TBM, or an upload of the data to an office away from the tunnel construction site. Both ways are either expensive or do not provide imaging results in real time. In addition, the basis for almost all imaging approaches is seismic migration, which demands significant computational power and further interpretation. We will thus focus on the development of a relatively simple but robust imaging processing technique with respect to the TSST-wave path. Goals of this study are to detect large scale geological structures ahead of the tunnel like fault zones, lithological boundaries, or large erratic blocks. No a priori information besides the measurement geometry shall be used. As a first step towards a reliable automatic interpretation of tunnel seismic data we will not attempt to classify or differentiate the kind of reflector. Instead, we will provide a stable and reliable distance estimate of the structure from the tunnel face. This can be the basis for further correlation with other information or the refinement of the imaging results.

First we demonstrate our strategy using 3D finite difference synthetic data. In a 3D full space model an evacuated tube (tunnel) is approaching two reflectors. At discrete tunnel face positions we model the seismic wave propagation excited by a point force source and record waves by only one receiver (Figure 1) which is a worst case scenario. In real tunnel surveys 2-4 receivers can be deployed along the tunnel wall. All together we simulate 56 shots.

The wave field excited by a hammer source applied at the tunnel wall and recorded by receivers mounted on the tunnel wall is usually dominated by the direct tunnel surface-wave (direct TS-wave) and its reflection at the tunnel face (reflected TS-wave, Figure 2a). In presence of a reflector with sufficient impedance contrast ahead of the tunnel face, we additionally observe the TSST-wave which arrives after the reflected TS-wave. For a measurement layout with constant distance of source and receiver to the tunnel face and in a homogeneous formation, both the direct and the reflected TS-wave appear in the seismogram sections at a constant time even if the tunnel construction is progressing (Figure 2b). However, with the decreasing tunnel face to reflector distance, the TSST-wave signals arrive earlier. In order to gain information on the tunnel face to reflector distance we simply have to isolate the TSST-wave signals. Figure 2 briefly illustrates the processing steps.

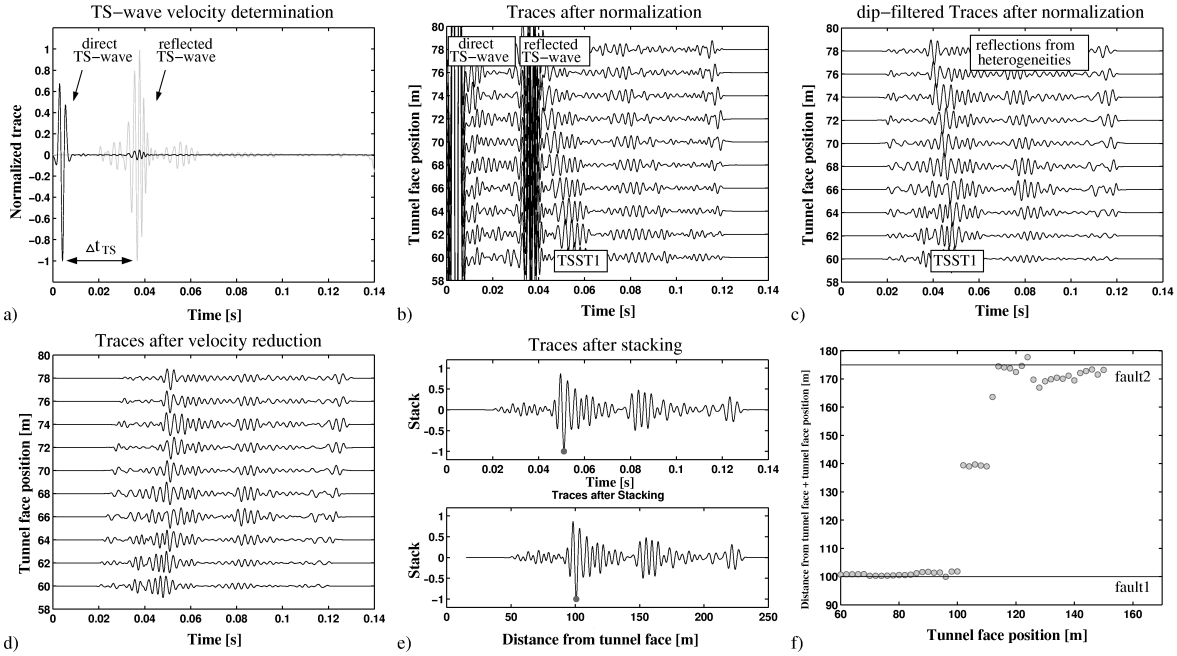

Figure 2: *Processing steps to detect geological structures ahead of the tunnel face using the simulated data. a) TS-wave velocity determination, first trace of synthetic tunnel seismic data (black line), first trace of tunnel seismic data after muting of direct TS-wave (gray line); b) window of 10 traces of non-processed synthetic tunnel seismic data illustrating the dominant direct TS-wave and the TS-wave reflected at the tunnel face; c) window of 10 traces of dip filtered synthetic tunnel seismic data. The TSST-wave is emphasized, direct and reflected TS-wave are suppressed; d) window of 10 traces of dip-filtered tunnel data after automatic formation S-wave velocity determination and correction; e) window of 10 traces of dip-filtered tunnel data after stacking, the maximum amplitude is marked; f) processing results of a moving window of 10 traces over the synthetic tunnel seismic data, the position of the peak amplitude of each stacked section is plotted.*

After applying all processing steps we automatically calculate the distance to the fault zone faces ahead of the tunnel. For better visibility, we sum the actual tunnel face position and the calculated fault to tunnel face distance. The position of a detected structure now refers to an absolute coordinate and should be constant with the progressing tunnel construction. As we can see from Figure 2f the first fault has been detected very well and while passing it, the imaging sequence locks in the second fault. With the decreasing distance to fault zone2 the prediction becomes more stable.

Field data Observations

Motivated by the good prediction results from synthetic tunnel data, we directly apply it to tunnel seismic field data acquired in the Piora adit near the Gotthard Base Tunnel (Switzerland). The Piora adit was drilled into the Penninic Gneiss zone heading towards the Piora Basin consisting of stable carbonatic sulfatic sedimentary rocks (Lüth et al., 2006). After completion of the tunnel, a receiver was anchored into the tunnel wall, and a pneumatic hammer source was applied at various offsets along the same tunnel wall side (Figure 3a). The common receiver gather is displayed in Figure 3b. The direct TS-wave is the dominant wave, and, apparently, formation heterogeneities south of the receiver cause reflections, which are visible parallel to the direct TS-wave as well. In comparison, the reflected TS-wave is weak, however stronger than the TSST arrivals marked by a black dashed line. Again, a dip filter is applied to the field data (Figure 3c). While significantly suppressing the disturbing reflections originated south of the receiver, the direct TS-wave could not be removed completely. Therefore, it has been muted separately. Considering that both the tunnel working front and the receiver are at a constant position, minor modifications had to be made to the processing sequence in order to handle the different measurement geometry. Since the reflected TS-wave is weak and separating direct and reflect TS-wave is difficult, we now automatically pick the first TS-wave arrivals in order to obtain the TS-wave velocity. Also, the apparent TSST-wave velocity from the common receiver gather corresponds directly to the formation S-wave velocity.

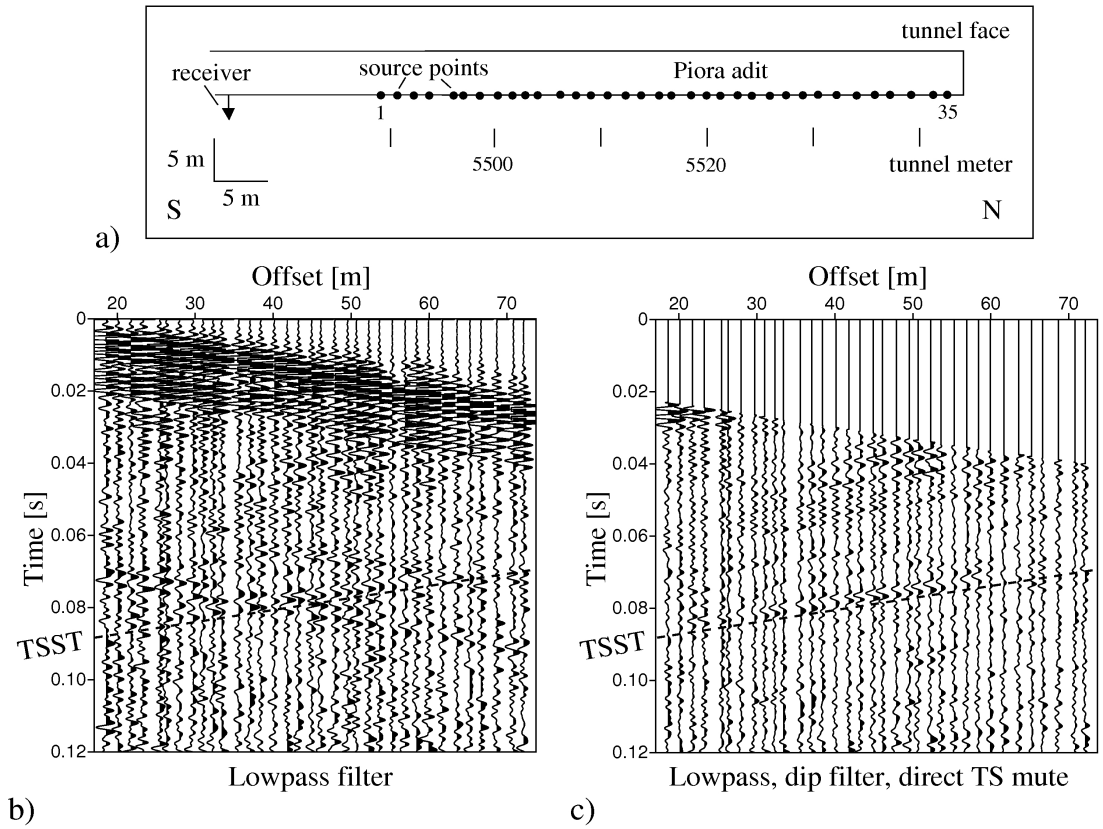

Figure 3: *a) Source and receiver geometry of a seismic survey in the Piora adit (top view. The receiver is marked by a triangle, the source points marked by circles are advancing towards the tunnel face; b) Common receiver gather (radial component) after applying a band pass filter (20-500 Hz), the amplitudes are gained linearly with time. The TSST-wave is marked by a dashed red line; c) Common-receiver gather (radial component) after applying a band pass filter (20-500 Hz), dip filter and muting of the direct TS-wave, the amplitudes are gained linearly with time.*

The results of the automated imaging processing are displayed in Figure 4a. In addition to the calculated distances (the tunnel face positions plus the offsets), we also plotted the determined formation S-wave velocity. The distance between the tunnel face and the Piora basin is stable at about 50 m for each window, and corresponds very well with both the rock quality index (RQD, Figure 4b)

and imaging results from a previous publication (Bohlen et al., 2007). Also, the formation S-wave velocities of about 3100 m/s obtained from each processing loop agree with results from previous surveys (Borm et al., 2003).

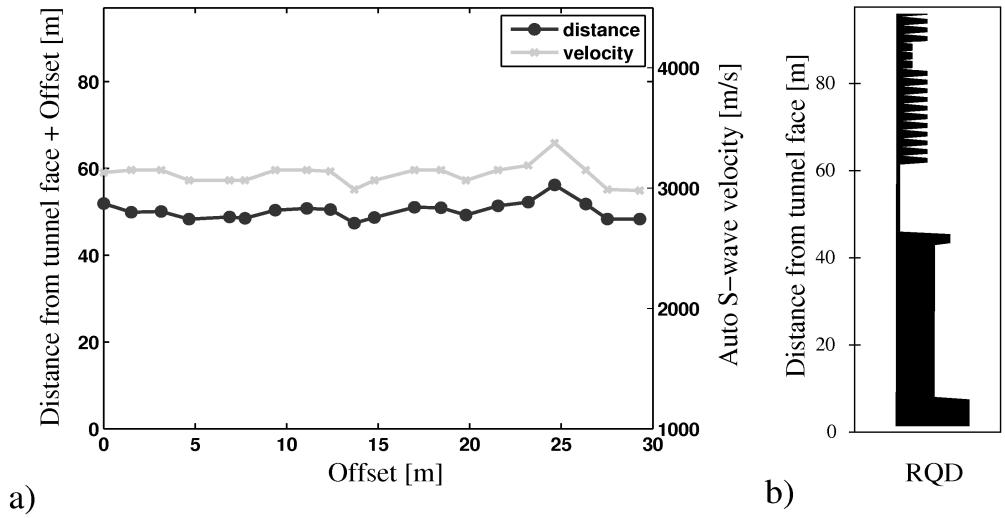

Figure 4: *a) Imaging processing results of the Piora adit field data (Figure 3), the automatically determined distance to the Piora basin from the tunnel face and the corresponding formation S-wave velocity are plotted. b) Rock quality index (RQD) profile ahead of the Piora adit (in direction of drilling), acquired from core samples (modified from Bohlen et al.,2007).*

Conclusions

Based on the concept of look-ahead prediction of the tunnel construction using tunnel surface-waves, we have designed a simple but robust detection technique for geological interfaces ahead of tunnel constructions. The main focus is the automatic detection of larger structures like faults or lithological boundaries, which can be correlated later with a priori information on the expected geological situation ahead of the tunnel. The imaging sequence basically focuses on the isolation and characterization (apparent velocity, arrival time) of TSST-waves. In both the synthetic and in field data examples, a sequence of frequency filter, dip filter, velocity reduction, and stacking within a moving window over the tunnel seismic data has shown the capability of estimating the reflector distance from the tunnel face. This estimate requires neither intensive processing and computational power, nor any a priori information and can be performed automatically. Since the tunnel look-ahead prediction concept using tunnel surface-waves is not limited to either hard rock or soft rock formation, the described imaging concept can be applied to most seismic tunnel surveys. Also, with minor modifications the imaging concept is expected to work for other seismic tunnel look-ahead prediction methods.

References

Bohlen, T., U. Lorang, W. Rabbel, G. Müller, R. Giese, S. Lüth, and S. Jetschny, 2007. Rayleigh-to-shear wave conversion at the tunnel face – from 3D-FD modeling to ahead-of-drill exploration: Geophysics, 72, T67–T79.

Jetschny, S., T. Bohlen, and D. De Nil, 2009. On the propagation characteristics of tunnel surface-waves for seismic prediction: accepted for publication in Geophysical Prospecting

Lüth, S., R. Giese, P. Otto, K. Krüger, S. Mielitz, T. Bohlen, and T. Dickmann, 2006. Seismic investigation of the Piora Basin using S-wave conversions at the tunnel face of the piora adit (Gotthard Base Tunnel): International Journal of & Mining Sciences, 45, 86–93.

Borm, G., R. Giese, P. Otto, F. Amberg, and T. Dickmann, 2003. Integrated seismic imaging system for geological prediciton during tunnel construction. ISRM 2003 – Technology roadmap for rock mechanics, South African Institute of Mining and Metallurgy.